

---

# Predicting Motion Plans for Articulating Everyday Objects

---

Anonymous Author(s)

Affiliation

Address

email

## Abstract

1 Mobile manipulation tasks such as opening a door, pulling open a drawer, or lifting  
2 a toilet seat require constrained motion of the end-effector under environmental  
3 and task constraints. This, coupled with partial information in novel environments,  
4 makes it challenging to employ classical motion planning approaches at test time.  
5 Our key insight is to cast it as a learning problem to leverage past experience  
6 of solving similar planning problems to directly predict motion plans for mobile  
7 manipulation tasks in novel situations at test time. To enable this, we develop a  
8 simulator, ArtObjSim, that simulates articulated objects placed in real scenes. We  
9 then introduce  $\text{IK}+\theta_0$ , a fast and flexible representation for motion plans. Finally,  
10 we learn models that use  $\text{IK}+\theta_0$  to quickly predict motion plans for articulating  
11 novel objects at test time. Experimental evaluation shows improved speed and  
12 accuracy at generating motion plans than pure search-based methods.

## 13 1 Introduction

14 As humans, when faced with everyday articulated objects as shown in Figure 1, we draw upon our  
15 vast past experience to successfully articulate them. We know to stand on the side as we pull open a  
16 oven, and where to lean on a door to push it open. Very rarely do we pull open a door onto our feet,  
17 or bump into the toilet while lifting a toilet seat. In this paper, we develop techniques that enable  
18 robots to similarly use past experience to *mine* and quickly *predict* strategies for articulating everyday  
19 objects in cluttered real environments.

20 Current work on articulating objects casts it as a motion planning problem: given a full scan of  
21 the environment, find a robot joint trajectory that leads the end-effector to track the trajectory that  
22 the grasp-point on the object should follow. This suffers from both a high-sensing cost and a high-  
23 planning cost. Building a full articulable 3D reconstruction of the environment for collision checking  
24 and planning is expensive and time consuming. At the same time, finding paths that conform to tight  
25 constraints on the end-effector trajectory while not colliding with self or surrounding obstacles or the  
26 articulating object is computationally hard. States that adhere to the given constraint form a measure  
27 zero set among the set of all states. This creates issues for sampling-based motion planners which  
28 can fail to sample states that satisfy the constraint, or must incur computation cost to project states to  
29 the constraint manifold [19, 4].

30 Rather than re-solving, from scratch, how to open a door every time we encounter one, our proposal  
31 is to build a repertoire of strategies based on past experience. This replaces the search in the high-  
32 dimensional motion plan space with the much simpler problem of selecting from a small family of  
33 good strategies, leading to gains in efficiency. Furthermore, this simpler search can be driven by  
34 whatever observation is readily available from on-board sensors through the use of machine learning.  
35 Our experiments demonstrate the effectiveness of casting this as a learning problem. Given a single  
36 RGB-D observation of an articulated object in cluttered real world scenes and associated end-effector

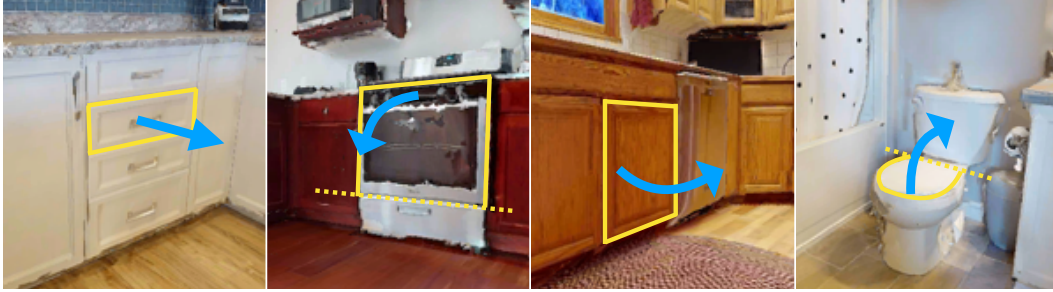


**Figure 1:** Household robots need to articulate everyday objects (*e.g.* pull open drawers, swing open cupboards, lift toilet seats). Such articulation involves applying forces onto the environment while maintaining relevant contact, such as with the drawer handle as we pull it open. This requires reasoning about the feasibility of the entire trajectory (*i.e.* points along the trajectory should not just be reachable, but it must be possible to continuously go from one point to the next). This paper develops datasets and techniques for learning models that can predict motion plans for such constrained motion planning problems with low sensing and planning costs.

37 pose trajectory to track, we can output motion plans that track the end-effector trajectory to within 1  
 38 cm error with just a few inverse kinematic calls. This, by far, outperforms the constrained motion  
 39 planning implementation for the projected state space method from the OMPL library [19, 42] which  
 40 fails to find any motion plans with less than 1cm tracking error even when given 15 minutes of  
 41 planning time. Our impressive performance is enabled by the following three key innovations.

42 First, we construct, ArtObjSim, a lightweight kinematic simulator for everyday articulated objects  
 43 placed in real scenes. Crucially, this simulator is derived from scans of *real-world* environments  
 44 (from HM3D dataset [35]). This retains the appearance and the cluttered environmental context of the  
 45 articulated objects. The simulator not only provides the experience to build the repertoire of strategies,  
 46 but also serves as the first of its kind benchmark for generating plans for articulating objects in real  
 47 environments. Our dataset consists of 2914 articulated object instances across 4 articulation types  
 48 (prismatic *e.g.* drawers, vertical hinge *e.g.* cabinets, horizontal up-hinge *e.g.* toilet lids, horizontal  
 49 down-hinge *e.g.* dishwashers) across 10 object categories in 97 scenes.

50 Second, rather than predicting a motion plans, that must conform to tight task constraints and are  
 51 hence hard to directly predict, we instead predict a *strategy* that can be efficiently decoded into a  
 52 motion plan using the articulation geometry. Our decoding process consists of *synchronously* solving  
 53 inverse kinematics (IK) problems for end-effector waypoints sampled along the given end-effector  
 54 trajectory. This synchronization is done by warm starting IK for the  $t^{\text{th}}$  time-step using solution  
 55 from the  $(t - 1)^{\text{th}}$  time-step. We call this decoding process Incremental Inverse Kinematics or  
 56 IIK. By directly optimizing to reduce end-effector pose error, IIK leads to low tracking errors. The  
 57 initialization for the first time step,  $\theta_0$ , serves as the strategy. Changing  $\theta_0$  changes the strategy and  
 58 generates a different motion plan. We find that this representation, IIK+ $\theta_0$ , is fast (motion plans  
 59 can be quickly decoded) and flexible (with the right  $\theta_0$  it can produce high-quality motion plans for  
 60 diverse objects in diverse situations).

61 Not all initializations would work well for all situations. Some might not be able to track the  
 62 end-effector accurately enough, some may lead to collisions, and others yet might violate the task  
 63 constraint when joint angles are interpolated for smooth execution. Thus, we need to find good  
 64 initializations for IIK+ $\theta_0$  at test time. Our third innovation, the use of a convolutional neural  
 65 network to predict good initializations for IIK+ $\theta_0$  (or equivalently, good strategies) from RGB image  
 66 observations, speeds up test time inference. We train this model on a dataset of object images labeled  
 67 with good initializations, as generated using our proposed ArtObjSim simulator. We are able to find  
 68 good solutions with only a few IK calls. This is much faster than sampling-based planning at test  
 69 time which would make tens of thousands of IK calls to project sampled states to the constraint set.  
 70 We also show that our method can work with predicted end-effector waypoints. Collected dataset,  
 71 ArtObjSim, and code will be made publicly available upon acceptance.

## 72 2 Related Work

73 **Motion planning under constraints** [19, 4] has been used to tackle object articulation problems,  
74 *e.g.* [36, 7, 34, 5, 27, 6, 44] among numerous other works. Researchers have tackled many aspects:  
75 design of task-space regions for expressing constraints on end-effectors [5], planning for base and arm  
76 motion separately [27], considering whole-body manipulation [6], reasoning about good locations to  
77 position the base through inverse reachability maps [44], and even casting it instead as a trajectory  
78 optimization or optimal control problem [9, 33, 40, 28]. All these approaches solve a new object  
79 articulation problem, from scratch, every time they encounter one. Consequently, they incur a high  
80 sensing and planning costs. Different from these works, our interest is in techniques to leverage  
81 experience with similar articulation problems in the past to quickly predict motion plans with low  
82 sensing and planning cost. Online system identification approaches [18, 16, 32, 31] that adapt plans  
83 using feedback have also been studied.

84 **Perception of articulated objects.** A body of work [47, 25, 17, 50, 29, 46, 45, 37, 1, 30, 21, 3, 2] has  
85 tackled the perception of *articulation* geometry for articulated objects. Given raw sensory input (RGB  
86 images, RGB-D images, depth images, point clouds, or meshes) the goal is to predict articulation  
87 parameters: *e.g.* articulation type (prismatic *vs.* hinge), segmentation of parts that independently  
88 articulate, axis of rotation / translation, points of interaction. Researchers have a) investigated the use  
89 of different input modalities [38, 29, 17, 25], b) built datasets for training models [30], c) designed  
90 unified output parameterizations [17], and d) designed novel neural architectures and representation  
91 [25, 50]. Researchers have also studied directly predicting sites for interaction [29] and trajectories  
92 that the robot end-effector should follow [47] to articulate the object. Our work is complementary,  
93 and focuses on converting articulation geometry, possibly predicted from any of these past models,  
94 into motion plans.

95 **Simulators for studying object articulation** have been challenging to build. Most past efforts use  
96 manually created *synthetic* scenes: AI2-THOR [22], Sapeins [49], ManipulaTHOR [8], ThreeD-  
97 World [10]. Habitat 2.0 [43] and iGibson [39] improve realism by manually aligning 3D models to  
98 real scenes, but are small in size (92 objects in 1 home and 500 objects in 15 homes respectively).  
99 Our proposed ArtObjSim simulator is unique in its focus, studying prediction of motion plans for  
100 everyday articulated objects, and scale, having 2900 articulated objects spread across 97 unique real  
101 world scenes. To our knowledge, ArtObjSim is the largest dataset, to date, for the study of motion  
102 planning performance for articulating everyday objects in everyday scenes.

103 **End-to-end RL approaches** can also be used to leverage prior experience for fast execution under  
104 partial information at test time [24, 48, 13]. However, the large sample complexity of learning policies  
105 through RL and the small number of environments available for training has prevented past works to  
106 show generalization results in novel environments. By leveraging classical components and scaling  
107 up learning, we are able to learn models that generalize to novel objects.

108 **Learning for motion planning** has been used to reduce the runtime of motion planning algorithms:  
109 [14, 41, 15]. Strudel *et al.* [41] learn obstacles representations for motion planning, while Ichter  
110 *et al.* [15, 14] use learning to bias sampling of states for motion planners. Our use of learning is  
111 similarly motivated, but we learn to predict low-dimensional strategies (that can be decoded into full  
112 motion plans) for constrained motion planning problems from visual input.

## 113 3 ArtObjSim: A Simulator for Everyday Articulated Objects in Real Scenes

114 We introduce ArtObjSim, a lightweight kinematic simulator for articulated objects placed in real  
115 scenes. ArtObjSim is built upon the HM3D dataset [35]. HM3D consists of 3D scans of real world  
116 environments. It offers both, realistic image renderings from real scenes, and access to the underlying  
117 3D scene geometry. ArtObjSim is made possible through 2D annotations of articulation geometry  
118 on images, which are then lifted to 3D to allow for a kinematic simulation of the articulated objects.  
119 To our knowledge, ArtObjSim is the first simulator that enables a systematic large-scale study of  
120 articulation of everyday objects in real world environments. We describe the steps involved in the  
121 construction of ArtObjSim.

122 **Annotating Articulation Geometry on Images.** The first step is to annotate 2D articulation geometry  
123 on images. 2D articulation geometry includes marking the extent, axis of articulation, articulation  
124 type, and interaction locations (handles). We collect annotations in two phases.

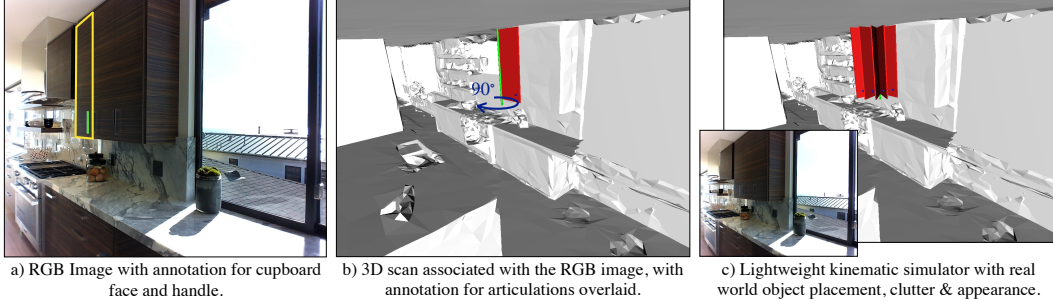


**Figure 2: Simulator development.** (a) We annotate RGB images inside 3D scans with 2D articulation geometry. (b) This is lifted to 3D using the underlying 3D geometry. (c) As a result we get simulators that can simulate articulated objects in realistic scenes.

125 In the first phase, we manually walk through the HM3D scenes to find kitchens and bathrooms and  
 126 identify locations that show articulation objects. We render out images from different viewpoints  
 127 from these locations for labeling.

128 In the second phase, we use an annotation service to obtain the necessary 2D labels. We obtain  
 129 annotations for the segmentation mask for the front face, handle locations, and articulation type  
 130 (prismatic *vs.* left hinge *vs.* right hinge *top* hinge *vs.* bottom hinge). See Figure 2(a) for an example  
 131 annotation. For most rectangular objects (*e.g.* drawers, cupboards, refrigerators) these three together  
 132 with the underlying 3D information from the mesh are sufficient to deduce the axis of articulation.  
 133 This doesn't work for toilets and we get additional labels for the axis of rotations (location where the  
 134 lid is attached). Toilet lids also don't have handles, we annotate and use the lid tip as the interaction  
 135 point.

136 We manually verify the annotation quality after each phase and fix or reject bad annotations. The  
 137 annotation procedure is fast and cost effective (\$0.5 per object instance).

138 **Extracting 3D Articulation Geometry from 2D Annotations.** We use the collected 2D annotations,  
 139 combined with the 3D scene geometry, to obtain a 3D simulation for each articulated object. For each  
 140 object, we fit a plane to the points within the segmentation mask on the depth image corresponding  
 141 to the RGB image. This gives us a 3D representation (a 3D rectangle) for the object face that  
 142 will undergo articulation. We project the 2D handle location onto this 3D plane to obtain the 3D  
 143 handle location. Articulation parameters are obtained from this 3D representation. We assume that  
 144 the prismatic objects pull out perpendicular to the face, and the hinged objects rotate about the  
 145 corresponding edge (top, bottom, left or right) of the 3D rectangle. As noted, toilet lids can't be  
 146 approximated as rectangles. We project the annotated 2D axis to the 3D plane. All annotations are  
 147 converted into the mesh coordinate frame using the transformations for the camera used to render out  
 148 the image. This defines all that we need to simulate the articulating object in 3D, see Figure 2(c).

149 **ArtObjSim Simulator.** As a result of the above two steps, we obtain kinematic simulations for  
 150 thousands of unique object instances placed in real 3D scenes. Not only can we simulate the object  
 151 (*i.e.* how the collision geometry will change as the object articulates or how will the end-effector need  
 152 to move), we also have a sense of the surrounding 3D geometry of the scene (*i.e.* the counter below  
 153 the cabinet), and can render out the RGB appearance of the object from multiple different views.

154 Table 1 shows dataset statistics. The dataset is diverse with close to 3000 object instances from across  
 155 97 scenes across 10 object categories and 4 articulation types. The dataset also includes a large  
 156 geometric variety *e.g.* cabinets high up above the counter and oven drawers very close to the ground.  
 157 This diversity, along with the fact that these objects are immersed in real scenes makes up problem  
 158 instances which have not been tackled extensively in the literature.

159 In Section 4, we will use ArtObjSim to design, train, and evaluate models for predicting motion plans  
 160 for articulating everyday objects. However, we anticipate ArtObjSim will be useful for many other  
 161 tasks. For example, predicting articulation parameters or end-effector waypoints from RGB images,  
 162 or for mining statistics about placement of articulated objects in kitchens to build generative models  
 163 for scene layout, or for building policies for mobile manipulation.

**Table 1:** Statistics for objects and scenes in Simulator for Everyday Articulated Objects in Context (ArtObjSim).

	Train	Val	Test	Total
# Scenes	70	17	10	97
# Unique Object Instances	2137	459	318	2914
# Prismatic (e.g. Drawer)	719	137	107	963
# Vertical Hinge (e.g. Cabinet)	1255	282	188	1725
# Horizontal Down-hinge (e.g. Oven)	163	40	23	226
# Horizontal Up-hinge (e.g. Toilet lid)	70	12	14	96

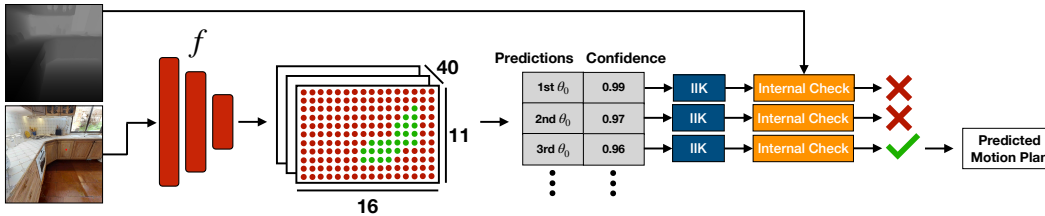


**Figure 3: Overview of MPAO (Motion Plans for Articulating Objects).** Given an RGB-D image of the object to be articulated (denoted with a red marker), we use a CNN to predict good initializations for incremental inverse kinematics (IIK). IIK uses end-effector trajectories to generate motion plans corresponding to each returned high-scoring initializations. Generated plans are tested for deviations from the intended trajectory, and collisions using the depth image. The first plan that succeeds these internal checks is returned.

## 164 4 Representing and Predicting Motion Plans

165 Given a single RGB-D image pair  $[I, D]$  of an articulated object, and a sequence of end-effector poses  
 166 necessary to articulate the object  $[\dots, w_t, \dots]$ , our next goal is to predict a motion plan, *i.e.* sequence  
 167 of joint angles  $[\dots, \theta_t, \dots]$  that bring the end-effector in the necessary pose to conduct the desired  
 168 articulation. Rather than re-solving each new problem instance from scratch using motion planning  
 169 under partial information, we pursue a machine learning approach that leverages past experience to  
 170 directly predict motion plans. A straight-forward application of machine learning doesn't work as the  
 171 predicted plans need to satisfy tight task constraints. Instead, we use machine learning to predict a  
 172 *strategy* which is decoded into a complete motion plan that adheres to the task constraints at hand.  
 173 We first describe what strategies are and how they are decoded in Section 4.1 and then describe how  
 174 we use them to predict motion plans from RGB images in Section 4.2.

### 175 4.1 Representing and Decoding Motion Plans

176 We represent motion plans as the initialization of a deterministic gradient-based solver that optimizes  
 177 joint angles to get the end-effector in the desired pose.

178 Our motion plan representation builds upon numerical inverse kinematics methods [26]. Inverse  
 179 kinematics (IK) is the process of obtaining joint angles that get the end-effector to a given desired  
 180 pose. Starting from some initial joint angles, a numerical IK solver iteratively updates the joint  
 181 angles using the Jacobian of the forward kinematics till a solution is found. As we are interested in  
 182 not one but a sequence of joint angles that track the given end-effector trajectory, we *incrementally*

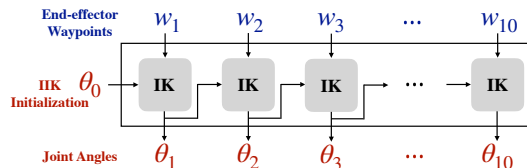


**Figure 4: Incremental Inverse Kinematics (IIK).** Given an initial configuration  $(\theta_0)$ , and a sequence of end-effector pose waypoints, IIK uses inverse kinematics (IK) to generate configurations that achieve the given end-effector waypoints. IK for subsequent steps is warm-started with IK solutions from the previous time step.

183 solve a sequence of inverse kinematic problems by initializing the inverse kinematic solver for the  $t^{\text{th}}$   
184 time-step with the solution from the  $(t - 1)^{\text{th}}$  time-step. We call this process, Incremental Inverse  
185 Kinematics or IIK, and show a block diagram in Figure 4.

186 Thus, IIK can be viewed as a *deterministic* process that converts a sequence of end-effector waypoints  
187 and an initial joint configuration  $\theta_0$  into a sequence of joint angles that realize the end-effector poses.  
188  $\theta_0$  can be thought of as *knob* that controls the motion plans that IIK generates. Varying  $\theta_0$  varies the  
189 motion plan generated. We use  $(\text{IIK}, \theta_0)$  as our representation for *strategies* that generate motion  
190 plans. Our experiments demonstrate that it is a flexible and efficient way to generate motion plans for  
191 articulating everyday objects, and outperforms both unconstrained and constrained motion planning  
192 approaches.

193 Note that  $\text{IIK}+\theta_0$ , shorthand for  $(\text{IIK}, \theta_0)$ , may not generate feasible motion plans for all inputs  
194  $\theta_0$ . Initializing from some  $\theta_0$  may not get the end-effector to where we want it to be, others might  
195 cause the end-effector to deviate too much from the desired trajectory when interpolating between  
196 waypoints, yet others might cause collisions with self or with the environment. We address this  
197 issue by *predicting* good  $\theta_0$ 's from the RGB image showing the articulated object as we describe in  
198 Section 4.2.

## 199 4.2 Predicting Motion Plans from Images

200 Our next step is to predict good initializations  $\theta_0$ 's for  $\text{IIK}+\theta_0$  from RGB images. As there can be  
201 more than one good  $\theta_0$  for each image, we adopt a classification approach. We work with a set of  
202 initializations  $\Theta$ . We train a function  $f(I, \theta_0)$  that classifies whether or not the use of  $\theta_0$  serves as a  
203 good initialization for IIK to achieve end-effector waypoints  $w$  without collisions. We provide details  
204 about the initialization set  $\Theta$ , function  $f$ , training data, and loss function to train  $f$ .

205 **Initialization set**  $\Theta$  comes from the Cartesian product of a set of robot base positions in  $\mathbb{R}^3$  and a set  
206 of 10 arm configurations. We use 704 base positions (sampled in a uniform  $1m \times 1.5m$  2D grid of  
207 base positions at a 10cm resolution at 4 different heights) and 10 arm configurations, resulting in  $\Theta$   
208 having 7040 elements. To acquire the 10 arm configurations, we sample 20 random configurations  
209 which satisfy the joint limits, and then select the 10 which give us the most successes across the  
210 dataset.

211 **Function**  $f$  is realized through a CNN with an ImageNet pre-trained ResNet-34 backbone [12]. We  
212 add 2 fully connected layers on the conv5 output to produce a 7040 dimensional representation. This  
213 is reshaped into an 80-dimensional spatial output of size  $11 \times 16$ . This is processed through another  
214 3 convolutional layers to produce a  $(10 \cdot 4) \times 11 \times 16$  tensor containing  $11 \times 16$  spatial output logits  
215 for each of the 10 arm configurations at each of the 4 heights.

216 **Training labels** are generated by decoding each candidate  $\theta_0$  into motion plans using IIK, and  
217 testing them for end-effector pose deviation, self-collision, collision with the static environment, and  
218 collision with the articulating object in our simulator from Section 3. Note that while testing the  
219 decoded motion plans, we interpolate between consecutive states to simulate how the plan will be  
220 executed in practice. This process generates a binary success label for each of the 7040 candidates in  
221  $\Theta$ . This is used to supervise the logits predicted by  $f$  via a binary cross-entropy loss.

222 **Training details.** Each articulated object instance in ArtObjSim comes with waypoints and ground  
223 truth labels as described above. We render multiple views for each articulated object to generate 30K  
224 images to train the function  $f$ .

225 Our full method, Motion Plans for Articulating Objects (MPAO), uses the learned function  $f$  to rank  
226 candidate initialization in  $\Theta$ . We go down the ranked list, decode them into motion plans using  
227 IIK, and return the first *feasible* plan (feasible meaning: accurately tracks the given waypoints and  
228 also doesn't collide with self or with the geometry visible in the depth image). See Figure 3 for an  
229 overview.

## 230 5 Experiments

231 Our experiments evaluate two aspects: a) the flexibility and decoding efficiency of our proposed  
232 motion plan representation from Section 4, and b) how effectively can we leverage RGB images to  
233 quickly convert end-effector poses to motion plans. For the former, we make comparisons to motion

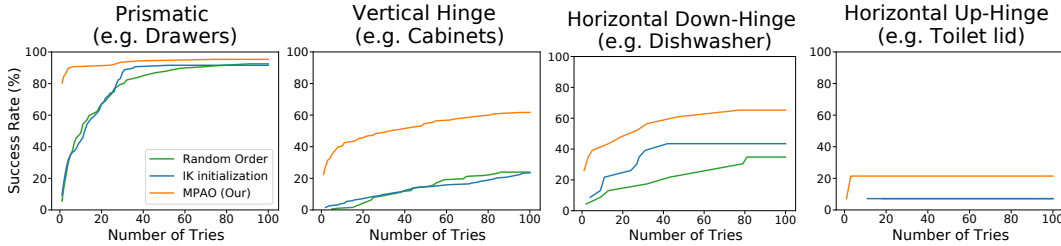


**Figure 5: Result plots.** We show success rate as a function of number of tries for the different articulation types. Our method, MPAO, that predicts good strategies based on visual input, achieves a higher success rate and generates solutions faster than pure search methods.

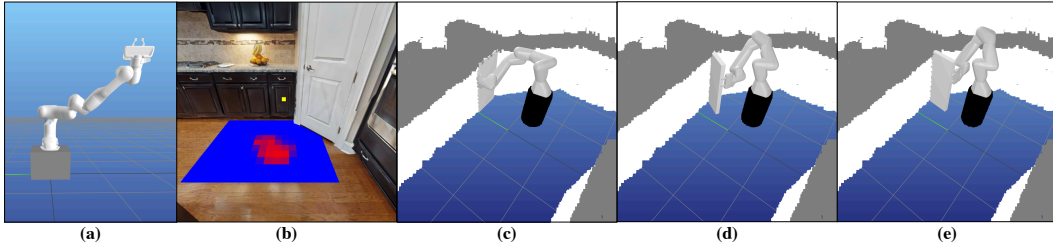


**Figure 6:** (a) One of the ten arm joint configurations from  $\Theta$  used for initialization. (b) Example of a cabinet from the dataset (indicated by the yellow marker), along with predictions for the configuration shown in (a) overlaid onto the image (warmer colors mean higher score). (c, d, e) Visualizations of a successful execution from one of the high-scoring locations.

234 planning, and for the latter we compare against variations that don't use the RGB image. We also  
 235 evaluate how our method works with predicted end-effector waypoints.

236 **Experimental Setup.** We leverage the geometry and appearance of articulated objects in real scenes  
 237 in our proposed ArtObjSim simulator for evaluation. We adopt the train, val, and test splits as noted  
 238 in Table 1. All instances from the same scene are in the same set. This allows us to measure how well  
 239 our models perform on novel held-out object instances. We work with the 7DOF Franka Emika Panda  
 240 robot. We assume that it can take one of 4 discrete heights (0.25m, 0.5m, 1.0m and 1.5m). While we  
 241 reason about where the base should be to conduct the motion, we assume that the base remains fixed  
 242 during execution. Leveraging base motion to better articulate objects is left to future work.

## 243 5.1 Motion Plan Representation

244 We evaluate the flexibility and decoding efficiency of our proposed motion planning representation.  
 245 More specifically, given a 10 time-step end-effector trajectory and complete collision geometry of the  
 246 situation, this evaluation measures the quality of the joint angle trajectory produced by our method.  
 247 We search for a good initialization  $\theta_0 \in \Theta$  for IIK and spits out the first solution that doesn't have  
 248 collisions (to self, surrounding environment, or the articulating object) and conforms to the given  
 249 tolerance in end-effector pose.

250 **Metric.** A predicted trajectory is considered successful if: a) it conveys the end-effector to the goal  
 251 pose within 1 cm and 0.01 radian, b) the resulting end-effector trajectory violates the task constraint  
 252 by less than 1 cm in translation and 0.01 radians in rotation for each time step, and c) it doesn't  
 253 cause collisions with self, the static environment, or the object as it articulates. Before measuring  
 254 deviations and collision-checking, we linearly interpolate the joint angle trajectories to bring all joint  
 255 angle changes to  $\leq 0.1$  radians.

256 **Results.** We report the success rate and time taken by our method for different articulation types in  
 257 Table 2. Prismatic drawers are easy: we can find solutions for 98.5% of the instances to within 0.01  
 258 cm, in as little as 2s of compute while only needing to try a median of 15 initializations. Vertical  
 259 hinged and horizontal down-hinged objects are harder: we are only able to solve 75% instances while  
 260 also needing to sample many more initializations, taking around 100s. Toilets are by far the hardest  
 261 because of the tight space in bathrooms.

262 **Comparison with other methods.** We also compared IIK+ $\theta_0$  to two other class of methods:

**Table 2: Motion planning for articulating objects under full information.** We measure the success rate and quality of successful plans generated by the different motion planning methods we considered. We note that  $\text{IK}+\theta_0$  is able to successfully generate plans quickly. Motion planning, both unconstrained and constrained, obtained a 0% success rate, and hence are omitted from the table, see Section 5.1 for more details.

Articulation Type	Performance		Speed	
	Success %	Deviation (cm)	#inits.	Time (s)
Prismatic ( <i>e.g.</i> Drawers)	98.5	0.01	15	2.48
Vertical Hinge ( <i>e.g.</i> Cabinets)	73.8	0.16	306	111.09
Horizontal Down-Hinge ( <i>e.g.</i> Dishwasher)	75.0	0.28	171	91.32
Horizontal Up-Hinge ( <i>e.g.</i> Toilet lid)	50.0	0.13	255	432.31

263 unconstrained and constrained motion planning, neither of which were able to find any successful  
 264 solutions in a tractable amount of time. For **unconstrained motion planning**, we used RRT-  
 265 connect [23] to find a path between a start and end joint configuration obtained using inverse  
 266 kinematics. While this always found a path, without any constraint on the intervening end-effector  
 267 poses, the path would always violate the 1-DOF constraint imposed by articulated object. This is  
 268 not surprising as the two poses are quite far from one another. To our surprise, even when these  
 269 poses are brought close to one another, by sampling 10 way-points along the trajectory, unconstrained  
 270 motion planning would still only return solutions that would wildly swing the end-effector around.  
 271 For **constrained motion planning**, we used the projected state space method from the OMPL  
 272 library [19, 42, 20]. It would find motion plans that conformed to the task constraint to some extent.  
 273 However, the minimum deviation was 2 cm, much more than the tolerance level needed for our  
 274 tasks, resulting again in a 0% success rate. We experimented with many different hyper-parameter  
 275 settings. Some worked better than others, but none were able to return any plans with lower than 2  
 276 cm deviations.

277 In summary,  $\text{IK}+\theta_0$  is effective at producing joint angles that conform to a given end-effector trajec-  
 278 tory. Finding a solution is still computationally expensive as it requires testing many initializations.  
 279 We address this using the prediction network  $f$ . We evaluate it next.

## 280 5.2 Motion Plan Prediction with Known Waypoints

281 Our next evaluation seeks to measure how quickly and accurately, we can predict motion plans for  
 282 articulated objects places in novel contexts as observed through RGB-D images. More specifically,  
 283 given an RGB-D image along with an end-effector trajectory, we measure the success rate of  
 284 predicting motion plans as a function of planning time. As in Section 5.1, we call a predicted motion  
 285 plan successful if it reaches the goal while violating the task constraint by less than 1 cm, 0.01 radians  
 286 and not colliding with self, the environment, and the articulating object. While the metric is the same,  
 287 the focus of this evaluation is to assess how well methods can cope with partial information from  
 288 RGB-D observations and their speed of generating solutions.

289 **Comparisons.** We compare against other search schemes for finding good  $\theta_0$  for IK. These baseline  
 290 schemes employ the same overall structure as our method (IK decoding followed by filtering based  
 291 on feasibility), but don't use any past experience (learned model) to rank initializations. We consider  
 292 two variants. *Random Order* uses the same set of initializations  $\Theta$  as our method, but evaluates them  
 293 in a random order. *IK initialization* conducts IK with 100 different initializations to generate arm  
 294 joint angles and base locations that reach the first end-effector waypoint.

295 **Results.** Figure 5 presents the success rate for different methods as a function of total number of  
 296 solutions tried for novel object instances in the test set. Across all articulation types, our method  
 297 dominates pure search baselines in success rate and speed. We are able to match baseline performance  
 298 for prismatic joints with  $3\times$  fewer tries, and obtain  $2.58\times$  the success rate of the baselines for vertical  
 299 hinges. This establishes the effectiveness of the learned model at predicting good initializations from  
 300 just RGB image observations. Figure 6 shows an example visualization. We also experimented with  
 301 a pure imitation learning approach that directly predicts the entire motion plan but weren't able to  
 302 train a model that generalized to novel instances in preliminary experiments.



### 303 **5.3 Motion Plan Prediction with Unknown Waypoints**

304 As a proof-of-concept, we have also integrated MPAO into an overall pipeline that doesn't require  
305 known waypoints. We experimented with drawers. We adapt Mask RCNN [11] to detect and  
306 predict drawer faces (segmentation mask) and handle locations (keypoints) using annotations from  
307 ArtObjSim. We converted them into end-effector waypoints using the depth image. This by itself  
308 gave an median error of 1.6cm. When using MPAO to track these predicted waypoints, we are able to  
309 predict plans that solve 39% drawers to within 1 cm error and 70% to within 5cm error.

## 310 **6 Conclusion**

311 We pursued a learning approach that uses past experience to quickly predict motion plans for  
312 articulating objects. We collected ArtObjSim, a large dataset that enables a kinematic simulation  
313 of everyday objects placed in real scenes. We designed IIK+ $\theta_0$ , a fast and flexible way to represent  
314 motion plans under end-effector constraints, and trained neural network models that leverage IIK+ $\theta_0$   
315 to quickly predict plans for articulating novel objects.

## References

- 316
- 317 [1] Ben Abbatematteo, Stefanie Tellex, and George Konidaris. Learning to generalize kinematic models to  
318 novel objects. In *CoRL*, pages 1289–1299, 2019.
- 319 [2] JKT Alexander Andreopoulos and John K Tsotsos. A framework for door localization and door opening  
320 using a robotic wheelchair for people living with mobility impairments. In *Robotics: Science and systems,  
321 Workshop: Robot manipulation: Sensing and adapting to the real world, Atlanta*, 2007.
- 322 [3] Dragomir Anguelov, Daphne Koller, Evan Parker, and Sebastian Thrun. Detecting and modeling doors  
323 with mobile robots. In *IEEE International Conference on Robotics and Automation, 2004. Proceedings.  
324 ICRA'04. 2004*, volume 4, pages 3777–3784. IEEE, 2004.
- 325 [4] Dmitry Berenson. *Obeying Constraints During Motion Planning*, pages 1–32. Springer Netherlands, 2018.
- 326 [5] Dmitry Berenson, Siddhartha Srinivasa, and James Kuffner. Task space regions: A framework for pose-  
327 constrained manipulation planning. *The International Journal of Robotics Research*, 30(12):1435–1460,  
328 2011.
- 329 [6] Felix Burget, Armin Hornung, and Maren Bennewitz. Whole-body motion planning for manipulation of  
330 articulated objects. In *ICRA*, pages 1656–1662, 2013.
- 331 [7] Sachin Chitta, Benjamin Cohen, and Maxim Likhachev. Planning for autonomous door opening with  
332 a mobile manipulator. In *2010 IEEE International Conference on Robotics and Automation*, pages  
333 1799–1806. IEEE, 2010.
- 334 [8] Kiana Ehsani, Winson Han, Alvaro Herrasti, Eli VanderBilt, Luca Weihs, Eric Kolve, Aniruddha Kembhavi,  
335 and Roozbeh Mottaghi. Manipulathor: A framework for visual object manipulation. In *Proceedings of the  
336 IEEE/CVF conference on computer vision and pattern recognition*, pages 4497–4506, 2021.
- 337 [9] Farbod Farshidian, Edo Jelavic, Asutosh Satapathy, Markus Gifftthaler, and Jonas Buchli. Real-time motion  
338 planning of legged robots: A model predictive control approach. In *ICHR*, pages 577–584, 2017.
- 339 [10] Chuang Gan, Jeremy Schwartz, Seth Alter, Martin Schrimpf, James Traer, Julian De Freitas, Jonas Kubilius,  
340 Abhishek Bhandwaldar, Nick Haber, Megumi Sano, et al. Threedworld: A platform for interactive multi-  
341 modal physical simulation. *arXiv preprint arXiv:2007.04954*, 2020.
- 342 [11] Kaiming He, Georgia Gkioxari, Piotr Dollár, and Ross Girshick. Mask r-cnn. In *ICCV*, pages 2961–2969,  
343 2017.
- 344 [12] Kaiming He, Xiangyu Zhang, Shaoqing Ren, and Jian Sun. Deep residual learning for image recognition.  
345 In *Proceedings of the IEEE conference on computer vision and pattern recognition*, pages 770–778, 2016.
- 346 [13] Daniel Honerkamp, Tim Welschehold, and Abhinav Valada. Learning kinematic feasibility for mobile  
347 manipulation through deep reinforcement learning. *IEEE RA-L*, pages 6289–6296, 2021.
- 348 [14] Brian Ichter, James Harrison, and Marco Pavone. Learning sampling distributions for robot motion  
349 planning. In *2018 IEEE International Conference on Robotics and Automation (ICRA)*, pages 7087–7094.  
350 IEEE, 2018.
- 351 [15] Brian Ichter, Edward Schmerling, Tsang-Wei Edward Lee, and Aleksandra Faust. Learned critical  
352 probabilistic roadmaps for robotic motion planning. In *2020 IEEE International Conference on Robotics  
353 and Automation (ICRA)*, pages 9535–9541. IEEE, 2020.
- 354 [16] Advait Jain and Charles C Kemp. Behaviors for robust door opening and doorway traversal with a  
355 force-sensing mobile manipulator. Georgia Institute of Technology, 2008.
- 356 [17] Ajinkya Jain, Rudolf Lioutikov, Caleb Chuck, and Scott Niekum. Screwnet: Category-independent  
357 articulation model estimation from depth images using screw theory. In *ICRA*, pages 13670–13677, 2021.
- 358 [18] Yiannis Karayiannidis, Christian Smith, Francisco Eli Vina Barrientos, Petter Ögren, and Danica Kragic.  
359 An adaptive control approach for opening doors and drawers under uncertainties. *IEEE Transactions on  
360 Robotics*, 32(1):161–175, 2016.
- 361 [19] Zachary Kingston, Mark Moll, and Lydia E Kavraki. Sampling-based methods for motion planning with  
362 constraints. *Annual review of control, robotics, and autonomous systems*, 1:159–185, 2018.
- 363 [20] Zachary Kingston, Mark Moll, and Lydia E. Kavraki. Exploring implicit spaces for constrained sampling-  
364 based planning. 38(10–11):1151–1178, September 2019.

- 365 [21] Ellen Klingbeil, Ashutosh Saxena, and Andrew Y Ng. Learning to open new doors. In *2010 IEEE/RSJ*  
366 *International Conference on Intelligent Robots and Systems*, pages 2751–2757. IEEE, 2010.
- 367 [22] Eric Kolve, Roozbeh Mottaghi, Winson Han, Eli VanderBilt, Luca Weihs, Alvaro Herrasti, Daniel Gordon,  
368 Yuke Zhu, Abhinav Gupta, and Ali Farhadi. AI2-THOR: An Interactive 3D Environment for Visual AI.  
369 *arXiv*, 2017.
- 370 [23] James J Kuffner and Steven M LaValle. RRT-connect: An efficient approach to single-query path planning.  
371 2000.
- 372 [24] Chengshu Li, Fei Xia, Roberto Martín-Martín, and Silvio Savarese. Hrl4in: Hierarchical reinforcement  
373 learning for interactive navigation with mobile manipulators. In *CoRL*, pages 603–616, 2020.
- 374 [25] Xiaolong Li, He Wang, Li Yi, Leonidas J Guibas, A Lynn Abbott, and Shuran Song. Category-level  
375 articulated object pose estimation. In *Proceedings of the IEEE/CVF conference on computer vision and*  
376 *pattern recognition*, pages 3706–3715, 2020.
- 377 [26] Kevin M Lynch and Frank C Park. *Modern robotics*. Cambridge University Press, 2017.
- 378 [27] Wim Meeussen, Melonee Wise, Stuart Glaser, Sachin Chitta, Conor McGann, Patrick Mihelich, Eitan  
379 Marder-Eppstein, Marius Muja, Victor Eruhimov, Tully Foote, John Hsu, Radu Bogdan Rusu, Bhaskara  
380 Marthi, Gary Bradski, Kurt Konolige, Brian Gerkey, and Eric Berger. Autonomous door opening and  
381 plugging in with a personal robot. In *2010 IEEE International Conference on Robotics and Automation*,  
382 pages 729–736. IEEE, 2010.
- 383 [28] Mayank Mittal, David Hoeller, Farbod Farshidian, Marco Hutter, and Animesh Garg. Articulated object  
384 interaction in unknown scenes with whole-body mobile manipulation. *arXiv preprint arXiv:2103.10534*,  
385 2021.
- 386 [29] Kaichun Mo, Leonidas Guibas, Mustafa Mukadam, Abhinav Gupta, and Shubham Tulsiani. Where2act:  
387 From pixels to actions for articulated 3d objects. *arXiv preprint arXiv:2101.02692*, 2021.
- 388 [30] Kaichun Mo, Shilin Zhu, Angel X. Chang, Li Yi, Subarna Tripathi, Leonidas J. Guibas, and Hao Su.  
389 PartNet: A large-scale benchmark for fine-grained and hierarchical part-level 3D object understanding. In  
390 *CVPR*, 2019.
- 391 [31] Keiji Nagatani and SI Yuta. An experiment on opening-door-behavior by an autonomous mobile robot  
392 with a manipulator. In *Proceedings 1995 IEEE/RSJ International Conference on Intelligent Robots and*  
393 *Systems. Human Robot Interaction and Cooperative Robots*, volume 2, pages 45–50. IEEE, 1995.
- 394 [32] Günter Niemeyer and J-JE Slotine. A simple strategy for opening an unknown door. In *Proceedings of*  
395 *International Conference on Robotics and Automation*, volume 2, pages 1448–1453. IEEE, 1997.
- 396 [33] Johannes Pankert and Marco Hutter. Perceptive model predictive control for continuous mobile manipula-  
397 tion. *IEEE RA-L*, pages 6177–6184, 2020.
- 398 [34] L Peterson, David Austin, and Danica Kragic. High-level control of a mobile manipulator for door  
399 opening. In *Proceedings. 2000 IEEE/RSJ International Conference on Intelligent Robots and Systems*  
400 *(IROS 2000)(Cat. No. 00CH37113)*, volume 3, pages 2333–2338. IEEE, 2000.
- 401 [35] Santhosh Kumar Ramakrishnan, Aaron Gokaslan, Erik Wijmans, Oleksandr Maksymets, Alexander Clegg,  
402 John M Turner, Eric Undersander, Wojciech Galuba, Andrew Westbury, Angel X Chang, Manolis Savva,  
403 Yili Zhao, and Dhruv Batra. Habitat-matterport 3d dataset (HM3d): 1000 large-scale 3d environments  
404 for embodied AI. In *Thirty-fifth Conference on Neural Information Processing Systems Datasets and*  
405 *Benchmarks Track (Round 2)*, 2021.
- 406 [36] T. Ruhr, J. Sturm, D. Pangercic, M. Beetz, and D. Cremers. A generalized framework for opening doors  
407 and drawers in kitchen environments. In *ICRA*, pages 3852–3858, 2012.
- 408 [37] R. B. Rusu, W. Meeussen, S. Chitta, and M. Beetz. Laser-based perception for door and handle identification.  
409 In *International Conference on Advanced Robotics*, pages 1–8, 2009.
- 410 [38] Radu Bogdan Rusu, Wim Meeussen, Sachin Chitta, and Michael Beetz. Laser-based perception for door  
411 and handle identification. In *2009 International Conference on Advanced Robotics*, pages 1–8. IEEE, 2009.
- 412 [39] Bokui Shen, Fei Xia, Chengshu Li, Roberto Martín-Martín, Linxi Fan, Guanzhi Wang, Claudia Pérez-  
413 D’Arpino, Shyamal Buch, Sanjana Srivastava, Lyne Tchapmi, et al. igibson 1.0: a simulation environment  
414 for interactive tasks in large realistic scenes. In *2021 IEEE/RSJ International Conference on Intelligent*  
415 *Robots and Systems (IROS)*, pages 7520–7527. IEEE, 2021.

- 416 [40] Jean-Pierre Sleiman, Farbod Farshidian, Maria Vittoria Minniti, and Marco Hutter. A unified mpc  
417 framework for whole-body dynamic locomotion and manipulation. *IEEE RA-L*, pages 4688–4695, 2021.
- 418 [41] Robin Strudel, Ricardo Garcia, Justin Carpentier, Jean-Paul Laumond, Ivan Laptev, and Cordelia Schmid.  
419 Learning obstacle representations for neural motion planning. *arXiv preprint arXiv:2008.11174*, 2020.
- 420 [42] Ioan A. Şucan, Mark Moll, and Lydia E. Kavraki. The Open Motion Planning Library. *IEEE Robotics &*  
421 *Automation Magazine*, 19(4):72–82, December 2012. <https://ompl.kavrakilab.org>.
- 422 [43] Andrew Szot, Alex Clegg, Eric Undersander, Erik Wijmans, Yili Zhao, John Turner, Noah Maestre, Mustafa  
423 Mukadam, Devendra Chaplot, Oleksandr Maksymets, Aaron Gokaslan, Vladimir Vondrus, Sameer Dharur,  
424 Franziska Meier, Wojciech Galuba, Angel Chang, Zsolt Kira, Vladlen Koltun, Jitendra Malik, Manolis  
425 Savva, and Dhruv Batra. Habitat 2.0: Training home assistants to rearrange their habitat. *arXiv preprint*  
426 *arXiv:2106.14405*, 2021.
- 427 [44] N. Vahrenkamp, T. Asfour, and R. Dillmann. Robot placement based on reachability inversion. In *ICRA*,  
428 pages 1970–1975, 2013.
- 429 [45] He Wang, Srinath Sridhar, Jingwei Huang, Julien Valentin, Shuran Song, and Leonidas J Guibas. Nor-  
430 malized object coordinate space for category-level 6d object pose and size estimation. In *CVPR*, pages  
431 2642–2651, 2019.
- 432 [46] Xiaogang Wang, Bin Zhou, Yahao Shi, Xiaowu Chen, Qinpeng Zhao, and Kai Xu. Shape2motion: Joint  
433 analysis of motion parts and attributes from 3d shapes. In *CVPR*, 2019.
- 434 [47] Ruihai Wu, Yan Zhao, Kaichun Mo, Zizheng Guo, Yian Wang, Tianhao Wu, Qingnan Fan, Xuelin Chen,  
435 Leonidas Guibas, and Hao Dong. VAT-Mart: Learning visual action trajectory proposals for manipulating  
436 3d articulated objects. *arXiv preprint arXiv:2106.14440*, 2021.
- 437 [48] Fei Xia, Chengshu Li, Roberto Martín-Martín, Or Litany, Alexander Toshev, and Silvio Savarese. Relmo-  
438 gen: Leveraging motion generation in reinforcement learning for mobile manipulation. *ICRA*, 2021.
- 439 [49] Fanbo Xiang, Yuzhe Qin, Kaichun Mo, Yikuan Xia, Hao Zhu, Fangchen Liu, Minghua Liu, Hanxiao Jiang,  
440 Yifu Yuan, He Wang, Li Yi, Angel X. Chang, Leonidas J. Guibas, and Hao Su. Sapien: A simulated  
441 part-based interactive environment. In *Proceedings of the IEEE Conference on Computer Vision and*  
442 *Pattern Recognition (CVPR)*, pages 11097–11107, 2020.
- 443 [50] Vicky Zeng, Timothy E Lee, Jacky Liang, and Oliver Kroemer. Visual identification of articulated object  
444 parts. In *IROS*, pages 2443–2450, 2021.